Climate and Weather of the Sun-Earth System (CAWSES): Selected Papers from the 2007 Kyoto Symposium,
Edited by T. Tsuda, R. Fujii, K. Shibata, and M. A. Geller, pp. 217–230.

Total solar irradiance variability: What have we learned about its variability from the record of the last three solar cycles?

Claus Fröhlich

Physikalisch-Meteorologisches Observatorium Davos, World Radiation Center,
CH–7260 Davos Dorf, Switzerland
E-mail: cfrohlich@pmodwrc.ch

Since November 1978 a set of total solar irradiance (TSI) measurements from space is available, yielding a time series of almost 30 years. Presently, there are three TSI composites available, called PMOD, ACRIM and IRMB, which are all constructed from the same original data, but use different procedures to correct for sensitivity changes. The PMOD composite is the only one which also corrects the early HF data for degradation. The origin of the differences between the three composite are discussed by comparison with the record of ERBE. For the discussion of the similarities and differences of the three cycles the PMOD composite is used. The most interesting feature is the low value of TSI at the present minimum which cannot be seen in proxies such as $F_{10.7}$, CaK and MgII indices. Thus, we see for the first time an effect on TSI which is not due to the direct effect of the superficial magnetic structures of solar activity.

1 Introduction

Since late 1978 total solar irradiance (TSI) measurements were made by different radiometers in space, HF on NIMBUS 7, ACRIM I on SMM, ERBE on ERBS, ACRIM II on UARS, SOVA on EURECA, VIRGO on SOHO, ACRIM III on ACRIM-Sat and since 2003 TIM on SORCE. Figure 1 shows these original time series and it is clear that not only the absolute values are quite different, especially at the beginning of the series, but there are also important differences between the series. This is e.g. obvious from comparison of early ACRIM-I with HF and is due to the fact that the original data from the HF radiometer cannot be corrected for degradation by internal means. These time series can be used for the construction of a TSI composite by shifting each series to a common level and merging them together. Presently there are three composites available, the first one was presented in 1997 at the IAU General Assembly in Kyoto by Fröhlich and Lean (1998b) and is now called PMOD composite (for the newest version see Fröhlich, 2006). A few months later the ACRIM composite was published by Willson (1997) which has been updated by Willson and Mordvinov (2003). Somewhat later a third composite, called IRMB, was presented

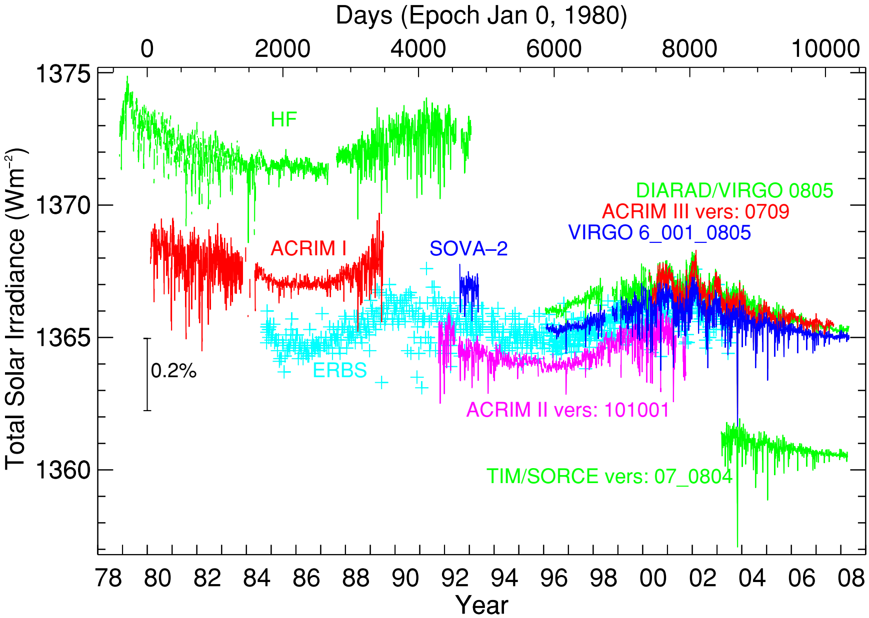

Fig. 1. Compared are daily averaged values of the Sun's total irradiance from radiometers on different space platforms as published by the instrument teams since November 1978. Note, that the VIRGO TSI is determined from both VIRGO radiometers (PMO6V and DIARAD), whereas the DIARAD TSI is only based on this one alone.

by Dewitte *et al*. (2004).[1]

2 Construction of TSI Composites

The ACRIM and IRMB composite use the data as published, whereas the PMOD composite introduces corrections of effects not considered in the original data sets. Already in the first versions of the PMOD composite corrections for the HF degradation were introduced (Fröhlich and Lean, 1998a, b). Similarly, the degradation of ACRIM-I during its first year was corrected for the effect of the rather short exposure time during the spin mode which was not taken into account in the original treatment by Willson and Hudson (1991). The two time series with the corrections mentioned were the basis for the composite of Fröhlich and Lean (1998a) during the period before the end of ACRIM-I in 1989 and remained unchanged up to version d40_61_0502. Since then the HF corrections have been re-determined (Fröhlich, 2006): after removal of all glitches throughout the mission a new HF time series was produced which is now corrected for the early increase, the degradation and the

[1]The composites are available from: PMOD at http://www.pmodwrc.ch/pmod.php?topic=tsi/composite/SolarConstant, ACRIM at http://www.acrim.com/Data%20Products.htm and IRMB at http://remotesensing.oma.be/solarconstant/sarr/SARR.txt.

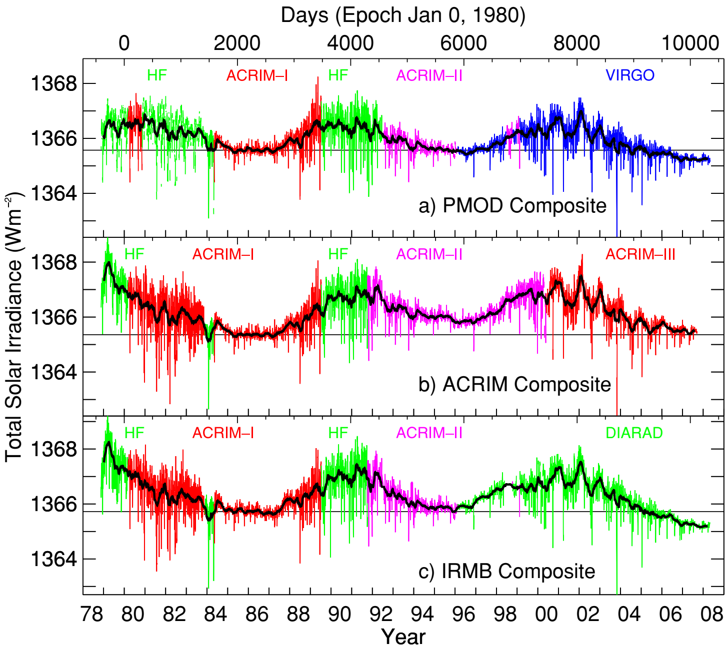

Fig. 2. Shown are the three composites: (a) PMOD (Fröhlich and Lean,1998b; Fröhlich, 2006), (b) ACRIM (Willson, 1997; Willson and Mordvinov, 2003) and (c) IRMB (Dewitte *et al.*, 2004).

long-term sensitivity increase over the full period of the NIMBUS-7 mission from November 1978 until January 1993.

Another problem for all composite constructions is how to bridge the so-called ACRIM gap between the end of ACRIM-I and the start of ACRIM-II, from June 1989 to October 1991. During this period daily values from HF and some 70 data points from ERBE with a sampling every 14 days are available. Already Lee III *et al.* (1995) revealed two slips in the HF data resulting in a total change of -0.68 W m^{-2} over this period which was confirmed by comparison with a model from the San Fernando group (Chapman *et al.*, 1996). Fröhlich (2000) re-analized this period and the overall change was also confirmed, but with a slightly different value of -0.58 W m^{-2}. With the corrected HF time series from Fröhlich (2006), there is no longer a need to treat the ACRIM gap separately, but the construction of the composite has become straightforward and internally consistent. The ACRIM composite neglects the corrections of the HF during the gap and this is the main reason for the claimed upward trend of TSI over the last three cycles (Willson and Mordvinov, 2003). The IRMB composite traces ACRIM-II to I via ERBE which results in an insignificant difference between the two minima. As IRMB uses ERBE data to trace ACRIM-I to ACRIM-II it yields a similar result for the difference between the minima in 1986 and 1996 as the PMOD composite. However, the IRMB times series during the ACRIM gap shows a strange

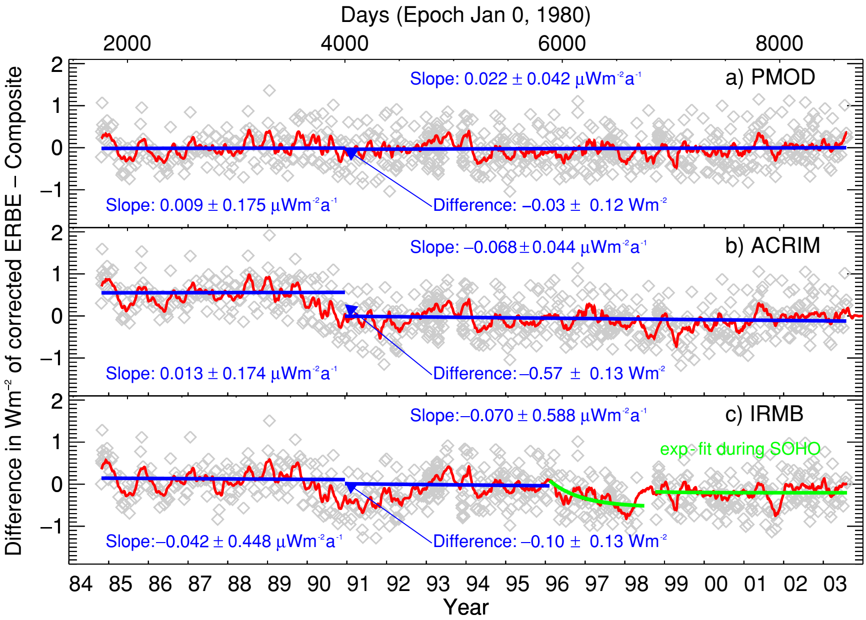

Fig. 3. Comparison of the three composites with the ERBE time series. ERBE is corrected for the early increase with the model parameters determined for ACRIM-I.

variation which comes from the fact that IRMB determines the composite as daily averages of the SARR[2] referred values of all available radiometers at that day.

After 1996 the PMOD uses version 6_001_0805 of the VIRGO data, which is updated to end of April 2008. How to derive the VIRGO data set is described in Fröhlich (2003) and in the online document[3]. The ACRIM composite uses for the same period a combination of ACRIM-II and III, whereas the IRMB composite uses the DIARAD/VIRGO data. In contrast to the official VIRGO TSI, the analysis of DIARAD/VIRGO is based on the measurements of DIARAD alone and the result is quite different. This is mainly due to the fact that their analysis implicitly neglects the non-exposure dependent increase of sensitivity which can only be determined by comparison with an independent radiometer.

The three composites are shown in Fig. 2. In terms of absolute scale the PMOD composite is referred to SARR, the ACRIM composite is on the scale of ACRIM-III and the IRMB refers first all data to SARR and then combines them without changing their level and thus the absolute scale. In order to get an independent view of the

[2]Space Absolute Radiometric Reference as defined by Crommelynck *et al.* (1995).

[3]http://www.pmodwrc.ch/pmod.php?topic=tsi/virgo gives some details about the corrections and presents links to the hourly and daily TSI data from VIRGO. Together with the official VIRGO TSI also the level 1.8 and 2 data for PMO6V and DiARAD are included, as well as the DIARAD/VIRGO data as determined by IRMB independently.

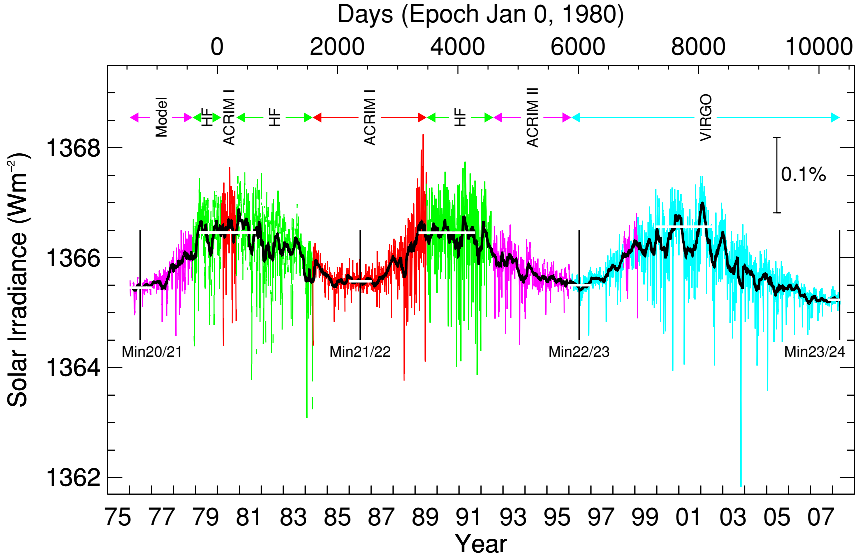

Fig. 4. Shown is the PMOD composite extended back to 1975 with the result of a 3-component proxy model as described in Section 4.

three composite we compare them with the ERBE data set, shown Fig. 3. As the ERBE radiometer is an ACRIM type and as the total exposure time is only 4 days we have applied the early increase correction determined for ACRIM-I (as described in Fröhlich, 2006). The most important result is that there is essentially no trend between the corrected ERBE time series and the PMOD composite, nor is there a significant step over the ACRIM gap. In the case of the IRMB composite the comparison with ERBE shows a similar exponential increase of sensitivity which has been identified during the evaluation of the VIRGO radiometry (Fröhlich, 2003) and is used in the evaluation of VIRGO TSI.

The above discussion of the three composites shows that the PMOD composite may possibly be the closest representative of the solar variability over the last 30 years. In order to have a more complete view of the behaviour of the Sun during the last three cycles the PMOD composite has been extended back to the minimum of 1975 with the result of a calibrated 3-component model as will be described in Section 4. This extended time series is shown in Fig. 4 and will be used in the following discussion.

3 Behaviour of TSI during the Last Three Solar Cycles

The changes of the maxima and minima from cycle to cycle are listed in Table 1. The other differences and similarities of the three cycles are more related to rotational variations. Cycle 21 and and 22 are similar, but quite different from cycle 23. The latter has less sunspots, as also shown by the lower maximum sunspot number of

Table 1. Listed are the values for the minima and maxima of the solar cycles 21–23 and the trend of the minima as change over the cycle relative to its amplitude. The amplitude is calculated from the difference between the maximum value and the mean of the two adjacent minima. The standard deviation are formal uncertainties of the corresponding average of the irradiance. For the maximum the average is over about 1000 days, for the minima over 350 days with the exception of the last minimum which covers yet only about 200 days.

		Cycle 21		Cycle 22		Cycle 23		
	Min	Max	Min	Max	Min	Max	Min	
Maxima		1366.49		1366.46		1366.39		W m^{-2}
Amplitude		0.980		0.921		1.029		W m^{-2}
StdDev		0.019		0.020		0.017		W m^{-2}
Minima	1365.46		1365.57		1365.50		1365.23	W m^{-2}
Dev. from Mean	0.015		0.131		0.060		−0.206	W m^{-2}
StdDev	0.006		0.006		0.008		0.006	W m^{-2}
Trend		11.8		7.7		−25.8		%

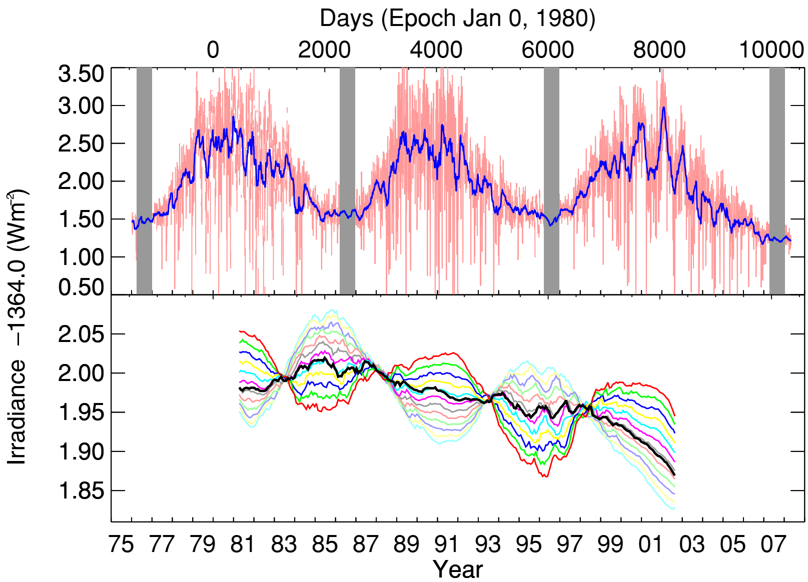

Fig. 5. The top panel shows the extended PMOD composite and the lower panel the cycle averaged long-term changes as in Lockwood and Fröhlich (2007). The red to light cyan lines show running means over intervals of 9 to 13 years. The black line gives the average length between the nodes (for details, see Lockwood and Fröhlich, 2007). Note the steeper decrease during the last cycle indicates that the general trend due to the diminishing amplitudes of the cycles is accentuated by the downward trend of TSI between the last minima.

about 115, compared to about 150 for the earlier cycles. On the other hand, this cycle has as many active regions as the others which is manifested by more peaks from the facular brightening which are not compensated by sunspot darkening. This is also the reason for the highest amplitude of this cycle relative to the others. Another point related to the sunspot numbers is the long-term change observed in cycle averaged TSI as shown in Lockwood and Fröhlich (2007, 2008) and updated in Fig. 5.

An important question is whether the recent downward trend is real and not an artefact of the analysis of the VIRGO data. For this we compare the PMOD composite with the ACRIM-II and III data over the whole cycle 23 and with TIM on SORCE since its launch in January 2003. Figure 6 shows that the comparison with ACRIM is quite noisy and shows some oscillatory behaviour with e.g. a 1-year periodicity, but with an overall trend of only 6.5 ppm/dec. The comparison with TIM is less noisy and shows a trend over the period 2003–2008 of 100 ppm/dec. It is interesting to note that the trend shown in this figure is from TIM version 8, whereas the corresponding trend of version 7 was only 6 ppm/dec. This may be partly due to the fact that an exponential function is fitted to the ratio of the operational TIM radiometer to the back-up ones, which is now no longer reproducing the steep decrease at the beginning of the mission. Moreover, the preliminary results from the re-analysis of

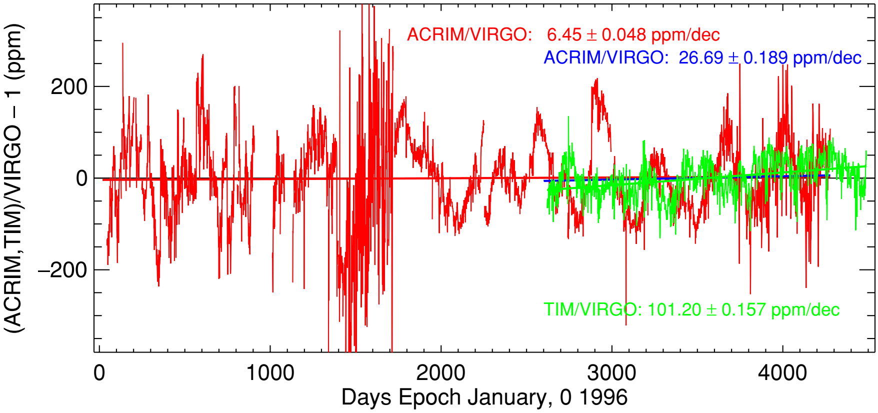

Fig. 6. Shown is the comparison of VIRGO TSI with ACRIM-II/III and TIM. TIM seems to indicate that there is a problem with the downward trend. For details see text, the conclusion is that this comparison may indicate that the trend as seen by VIRGO may be somewhat too large, maybe not 26% of the cycle amplitude, but still certainly more than 18%.

the VIRGO radiometry indicate that the cycle amplitude may be somewhat underestimated which would also reduce the slope of the ratio TIM/VIRGO. The trend of the ratio to ACRIM over the same period as for TIM is also increased, but amounts only to about one quarter of the one seen by TIM. Taking these results as an indication of the uncertainty we may attribute to the observed trend an uncertainty of about 50 ppm/dec. Thus the downward trend during cycle 23 maybe somewhat overestimated by the VIRGO data, but it is still around 18%. So, we are confident that the downward trend is real and we have to find a physical explanation, which must be different from changes of the upper atmosphere due to surface magnetism.

4 Proxy Models and Reconstructions

Proxy models are based on the photometric sunspot index (PSI) and some proxy for the influence of faculae and network. PSI was first described by Hudson *et al.* (1982) and is based on time-dependent information about sunspot areas and locations determined from ground-based white light images made from 1882 to 1976 by the Greenwich Observatory, and most recently by the U.S. Air Force operational Solar Observation Optical Network (SOON) sites.[4] Here we use an improved version of the same basic algorithm Fröhlich *et al.* (1994) together with a size dependent contrast from Brandt *et al.* (1994). The explicit calculation of a facular index PFI analogous to PSI is also possible (Lean *et al.*, 1998) but more difficult because faculae have lower contrasts in the visible spectrum and more fragmented areas than sunspots. This motivates the use of alternative facular indices such as the Mg-II index, which consists

[4]The observations of the sunspot regions are available from the National Geophysical Data Center (NGDC) operated by the National Oceanographic and Atmospheric Administration (NOAA) at Boulder, Colorado, http://www.ngdc.noaa.gov/stp/SOLAR/ftpsunspotregions.html.

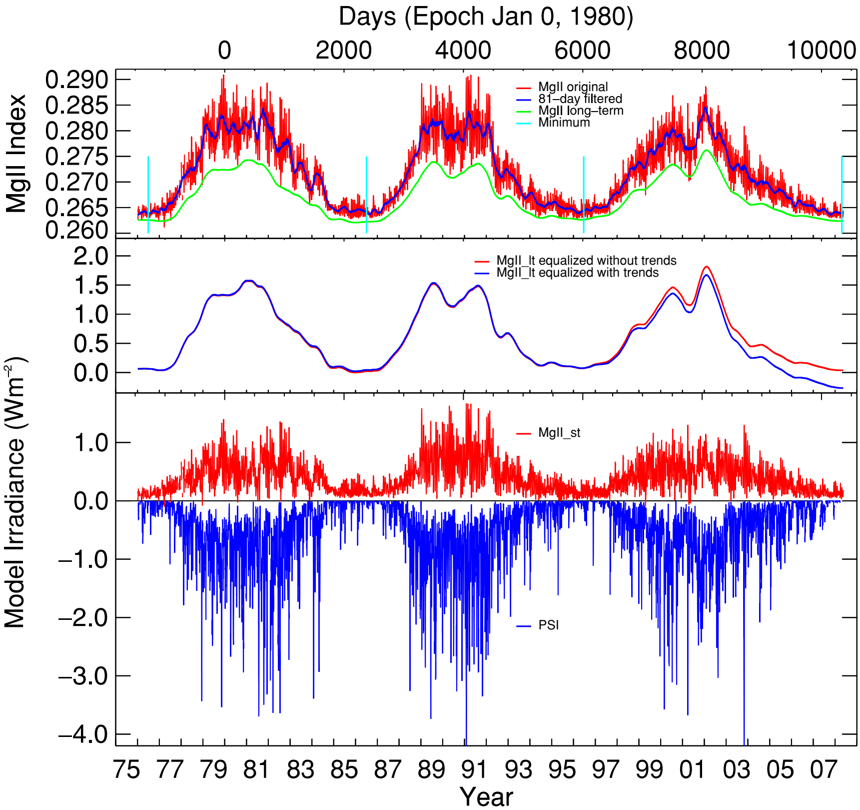

Fig. 7. The top panel shows the composite MgII index (red) and the long-term part determined as a lower envelope of short-term variation mainly due to the passage of faculae. The lower two panels show the calibrated indices: long-term MgII, short-term MgII together with PSI. The vertical lines on the top panel indicate the time of the solar cycle minima.

of the ratio of the core and wing fluxes and minimizes the influence of instrumental drifts. The line cores originate in the chromosphere where bright features have greater contrast than their photospheric counterparts (a factor of 2 versus a few percent for an active region), and the flux measurements automatically integrate emission over the full disk. One disadvantage is that chromospheric and photospheric radiances have different center-to-limb dependence of emission and contrast. By following an active region passage without a sunspot we observe in TSI two maxima at about 4–5 days before and after the central-meridian passage with a minimum at the central meridian, and in contrast the MgII index shows one peak at the central meridian. A method to take this difference into account has been presented earlier by Fröhlich (2004), but here we make no correction for this effect because the improvement is only marginal for the present discussions. The composite MgII index from Viereck *et al.* (2004)

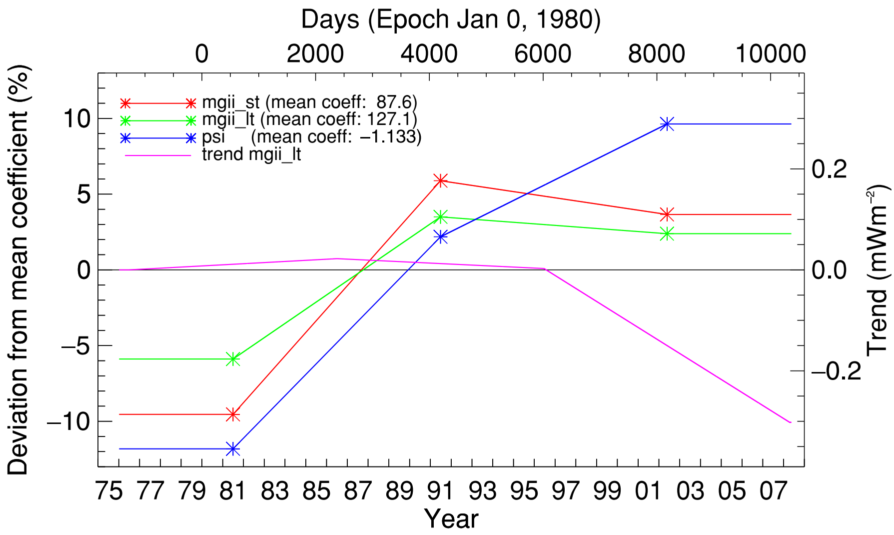

Fig. 8. Shown are the changes of the coefficients determined for each cycle relative to there mean value. These changes are then used to 'correct' the long and short-term MgII and PSI for further analysis. Also shown are the trends needed to be introduced to account for the changes in TSI not represented by the MgII index, nor PSI.

is used which has been recently corrected during cycle 23 and updated until 2008 by Viereck *et al*. (2008). This composite has been extended back to spring 1976 with HeI equivalent width data, calibrated against MgII index over the rest of cycle 21. The MgII index is shown in the top panel of Fig. 7. From comparison of the MgII and TSI time series it is clear that the recent downward trend cannot be explained by a model based on such proxies. This is not only true for MgII index, also CaK index, the radio flux at 10.7 cm and similarly the sunspot number do not show any substantial changes of the values at solar minima. For $F_{10.7}$ this is true back to the beginning of the measurements in the late forties and for the CaK index back to 1915. This means that the surface manifestations of activity such as sunspots, faculae and network, which change the temperature structure of the upper solar atmosphere, explain only the cycle variations of TSI, but not the trends from minimum to minimum. These trends may still be related to activity, by e.g. temperature changes of the photosphere. TSI is with 0.07%/K quite sensitive to such changes whereas the for UV radiation at e.g. 200 nm a change of 0.22%/K is negligible compared to the effect of chromospheric changes during a cycle.

Moreover, there may be a difference of the effect influencing the variability over a full solar cycle and over only solar rotation which is directly linked to the passage of active regions. So, the MgII index is separated into a long-term part which is determined as the lower envelope of the index as shown in Fig. 7. The short-term is then obtained by subtracting the so determined long-term from the observed MgII index.

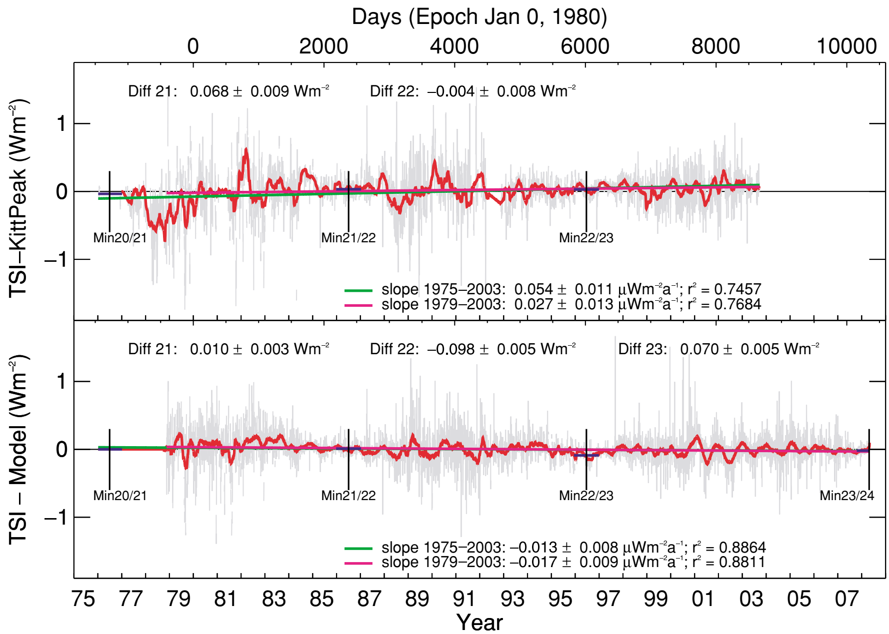

Fig. 9. The top panel shows the comparison between TSI and the reconstruction by Wenzler *et al*. (2006) and the bottom panel the one between TSI and corrected 3-component proxy model with trends for each cycle added.

The long-term on the other hand is varying slowly and may be due to changes of the network inside and outside active regions in the course of a cycle. Multiple regression of the three components against TSI is used to 'calibrate' the model. However, as the MgII index has essentially no change of the minima, we need to add a fourth component to account for trends between the minima of each cycle. In a first step each cycle is fitted separately in order to account for possible changes of e.g. the contrast of sunspots and faculae. The results are shown in Fig. 8. As in earlier analysis (e.g. Fröhlich and Lean, 2004) we find different coefficients for the long- and short-term MgII index which may be explained by a different specific contrast of faculae and network (Ortiz, 2005) and thus may indicate that the solar-cycle modulation is indeed due to changes of the network and not due to the faculae and sunspots alone. The differences between the three cycles show a steady increase of all parameters relative to their mean—especially between cycle 21 and 22 and somewhat less between 22 and 23. Albeit the coefficients change the ratios of the short-term to the long-term coefficients stay about constant at 1.46±0.05. Also the contrasts for sunspots and faculae seem to change from cycle to cycle, but again not so much their ratio. Both observations are by itself very interesting and may help to understand better the influence of surface magnetism. Now we adjust the short and long-term MgII and PSI to the mean coefficients from Fig. 8, add the trends and redo the calibration against TSI. The result of this adjusted model is shown as comparsion with TSI in the bottom panel of Fig. 9. The correlation is extremely high and it explains 86% of the variance. This indicates that not only the effect of faculae, network and sunspots are quite different during the three cycles, but also that different trends for each cycle are necessary.

Another way to reconstruct TSI is based on the identification of sunspot (umbra, penumbra and pores) pixels from white light images and of quiet, network and facular pixels from the magnetograms (see e.g. Wenzler *et al.*, 2005). Together with a contrast (see e.g. Krivova *et al.*, 2003) the radiance of each pixel is determined and summed up to yield the irradiance. The pixels from the sunspot and pores are subtracted from the magnetograms and the remaining pixels represent faculae and network for which a filling factor is defined which depends linearly on the magnetic field in the pixel up to a saturation field after which it is set to one. This saturation field is the only free parameter in this type of reconstruction which is determined by calibration against the PMOD composite as 340 G for the Kitt-Peak magnetograms (Wenzler *et al.*, 2005, 2006). This reconstruction covering the period of the composites from the beginning of the measurements of TSI up to the maximum of solar cycle 23 can also be used to compare the three composites. As with ERBE the best agreement is found for the PMOD composite explaining 77% of the variance (see Fig. 9, top panel). This is a rather high correlation for the simple assumptions with only one free parameter on which the reconstruction is based. On the other hand there also are important deviations which explain the lower correlation than the one achieved by the corrected 3-component model with trends. They come mainly from the fact that the saturation field is determined from the data of cycle 23 and obviously the level of agreement is much lower for the ascending parts of cycle 21 and 22 than for the ascending part of cycle 23. Part of this discrepancy may be removed if each cycle would be calibrated separately as in the proxy model. These reconstructions fail also to explain minimum-to-minimum trends, similar to the other chromospheric proxies. The reason why this reconstruction fits the TSI composite quite well is due to the fact that there was only a small trend over cycle 22 and that the comparison is limited to the period from maximum of cycle 21 to the maximum of 23.

5 Conclusions

The most important result is that TSI shows trends from minimum to minimum which cannot be reproduced by proxies for the brightening due to magnetic surface structures, such as the 10.7 cm radio flux, CaK and MgII indices or the ones deduced from magnetograms. They vary from minimum to minimum at most by a few percent whereas TSI changed during cycle 23 by 18% or more. As the reconstructions and proxy models represent very well the irradiance changes during a cycle of TSI and the UV radiation they cannot explain the long-term trends. This in turn means also that the UV radiation has probably no long-term trend even back to the Maunder Minimum, only changes of the cycle amplitude which can most probably be well represented by the amplitude of the sunspot number. On the other hand TSI shows a long-term trend which could be due to a change of the temperature of the photosphere, which changes TSI but not the UV radiation. This temperature change may also be related to the magnetic field emerging during a cycle and thus may well be related to the long-term changes of the amplitude of the sunspot number also. So, a long-term trend for TSI on top of the amplitude changes of the individual cycles is highly probable. But the same long-term trend cannot be applied to the UV irradiance, which shows only an important variation related to the cycle amplitude.

Acknowledgments. Continued support of solar irradiance research at PMOD/WRC by the Swiss National Science Foundation is greatly acknowledged. Thanks are extended to the VIRGO team for supporting the experiment on SOHO, a cooperative ESA/NASA mission, and to the ACRIM and SORCE teams for still unpublished data.

References

Brandt, P. N., M. Stix, and H. Weinhardt, Modelling solar irradiance variations with an area dependent photometric sunspot index, *Sol. Phys.*, **152**, 119–124, 1994.

Chapman, G. A., A. M. Cookson, and J. J. Dobias, Variations in total solar irradiance during solar cycle 22, *J. Geophys. Res.*, **101**, 13541–13548, 1996.

Crommelynck, D., A. Fichot, R. B. Lee III, and J. Romero, First realisation of the space absolute radiometric reference (SARR) during the ATLAS 2 flight period, *Adv. Space Res.*, **16**(8), 17–23, 1995.

Dewitte, S., D. Crommelynck, S. Mekaoui, and A. Joukoff, Measurement and uncertainty of the long-term total solar irradiance trend, *Sol. Phys.*, **224**, 209–216, doi:10.1007/s11207-005-5698-7, 2004.

Fröhlich, C., Observations of irradiance variability, *Space Sci. Res.*, **94**, 15–24, 2000.

Fröhlich, C., Long-term behaviour of space radiometers, *Metrologia*, **40**, 60–65, 2003.

Fröhlich, C., Solar irradiance variability, in *Geophysical Monograph 141: Solar Variability and its Effect on Climate*, Chapter 2: Solar Energy Flux Variations, 97–110, AGU, Washington DC, USA, 2004.

Fröhlich, C., Solar irradiance variability since 1978: Revision of the PMOD composite during solar cycle 21, *Space Sci. Res.*, **125**, 53–65, doi:10.1007/s11214-006-9046-5, 2006.

Fröhlich, C. and J. Lean, The sun's total irradiance: Cycles and trends in the past two decades and associated climate change uncertainties, *Geophys. Res. Lett.*, **25**, 4377–4380, 1998a.

Fröhlich, C. and J. Lean, Total solar irradiance variations: The construction of a composite and its comparison with models, in *IAU Symposium 185: New Eyes to See Inside the Sun and Stars*, edited by F. L. Deubner, J. Christensen-Dalsgaard, and D. Kurtz, 89–102, Kluwer Academic Pub., Dordrecht, The Netherlands, 1998b.

Fröhlich, C. and J. Lean, Solar radiative output and its variability: Evidence and mechanisms, *Astron. Astrophys. Rev.*, **12**, 273–320, doi:10.1007/s00159-004-0024-1, 2004.

Fröhlich, C., J. M. Pap, and H. S. Hudson, Improvement of the photometric sunspot index and changes of disk-integrated sunspot contrast with time, *Sol. Phys.*, **152**, 111–118, 1994.

Hudson, H. S., S. Silva, M. Woodard, and R. C. Willson, The effects of sunspots on solar irradiance, *Sol. Phys.*, **76**, 211–218, 1982.

Krivova, N. A., S. K. Solanki, M. Fligge, and Y. C. Unruh, Reconstruction of solar total and spectral irradiance variations in cycle 23: is solar surface magnetism the cause?, *Astron. Astrophys.*, **399**, L1–L4, 2003.

Lean, J. L., J. Cook, W. Marquette, and A. Johannesson, Magnetic sources of the solar irradiance cycle, *Astrophys. J.*, **492**, 390–401, 1998.

Lee III, R. B., M. A. Gibson, R. S. Wilson, and S. Thomas, Long-term total solar irradiance variability during sunspot cycle 22, *J. Geophys. Res.*, **100**, 1667–1675, 1995.

Lockwood, M. and C. Fröhlich, Recent oppositely directed trends in solar climate forcing and the global mean surface air temperature, *Proc. R. Soc. A*, **463**, 2447–2460, doi:10.1098/rspa.2007.1880, 2007.

Lockwood, M. and C. Fröhlich, Recent oppositely-directed trends in solar climate forcings and the global mean surface air temperature: II. different reconstructions of the total solar irradiance variation and dependence on response timescale, *Proc. R. Soc. A*, **464**, 1367–1385, doi:10.1098/rspa.2007.0347, 2008.

Ortiz, A., Solar cycle evolution of the contrast of small photospheric magnetic elements, *Adv. Space Res.*, **35**, 350–360, doi:10.1016/j.asr.2005.03.014, 2005.

Viereck, R. A., L. E. Floyd, P. C. Crane, T. N. Woods, B. G. Knapp, G. Rottman, M. Weber, L. C. Puga, and M. T. DeLand, A composite Mg II index spanning from 1978 to 2003, *Space Weather*, **2**, S10005, doi:10.1029/2004SW000084, 2004.

Viereck, R. A. *et al.*, Update of the composite Mg II index, 2, 2008 (personal communication, will be published).

Wenzler, T., S. K. Solanki, and N. A. Krivova, Can surface magnetic fields reproduce solar irradiance variations in cycles 22 and 23?, *Astron. Astrophys.*, **432**, 1057–1061, doi:10.1051/0004-6361:20041956, 2005.

Wenzler, T., S. K. Solanki, N. A. Krivova, and C. Fröhlich, Reconstruction of solar irradiance variations in cycles 21–23 based on surface magnetic fields, *Astron. Astrophys.*, **460**, 583–595, doi:10.1051/0004-6361:20065752, 2006.

Willson, R. C., Total solar irradiance trend during solar cycles 21 and 22, *Science*, **277**, 1963–1965, 1997.

Willson, R. C. and H. S. Hudson, The Sun's luminosity over a complete solar cycle, *Nature*, **351**, 42–44, 1991.

Willson, R. C. and A. V. Mordvinov, Secular total solar irradiance trend during solar cycles 21–23, *Geophys. Res. Lett.*, **30**, 1199, doi:10.1029/2002GL016038, 2003.